

Supporting Information:

P-C Bond Cleavage Induced Ni(II) Complexes Bearing Rare-earth-Metal-Based Metalloligand and Reactivities Toward Isonitrile, Nitrile and Epoxide.

Peng Cui,^{*,†,‡} Xia Huang,[†] Jun Du,[†] Zeming Huang[†]

[†] Key Laboratory of Functionalized Molecular Solids, Ministry of Education, Anhui Laboratory of Molecule-Based Materials, College of Chemistry and Materials Science, Anhui Normal University, Wuhu, Anhui 241002, P. R. China.

[‡] Key Laboratory of Organic Synthesis of Jiangsu Province, Soochow University, Suzhou 215123, P. R. China

Table of Contents:

1. Spectroscopic Data	2
1.1 NMR spectra.....	2
1.2. IR Spectra.....	16
2. X-ray Crystallography	17
3. References	20

1. Spectroscopic Data

1.1 NMR spectra

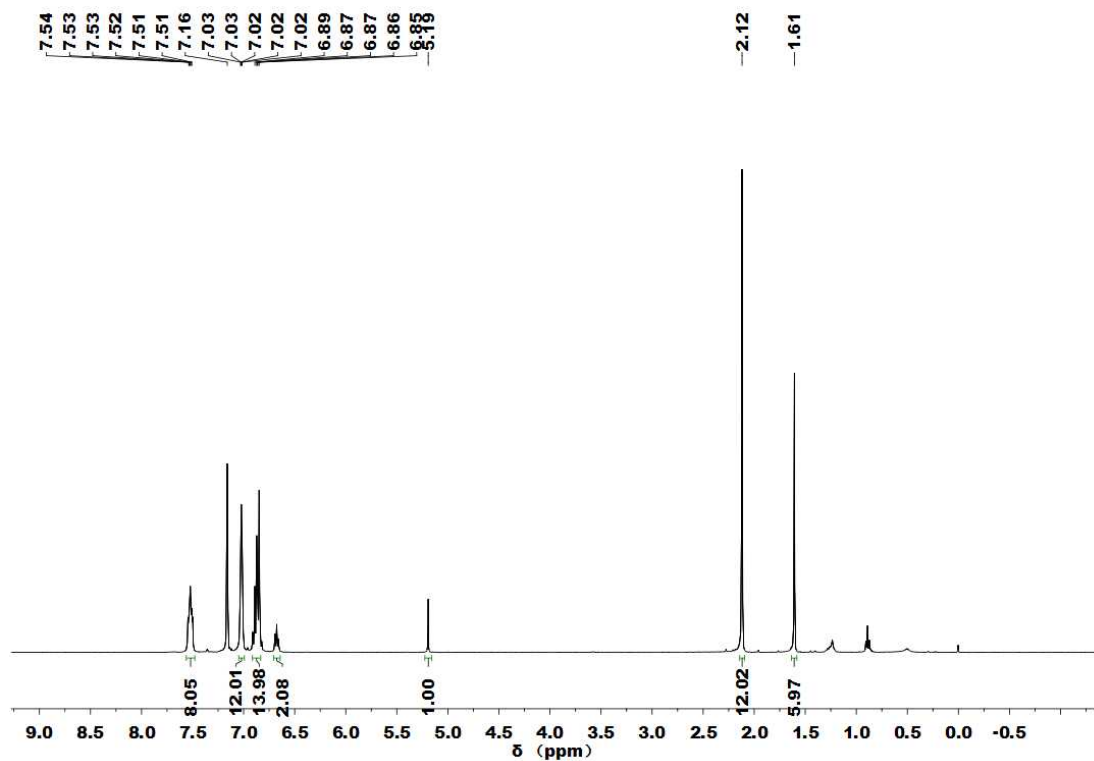


Figure S1. ^1H NMR spectrum of **1** in C_6D_6 at 25 °C.

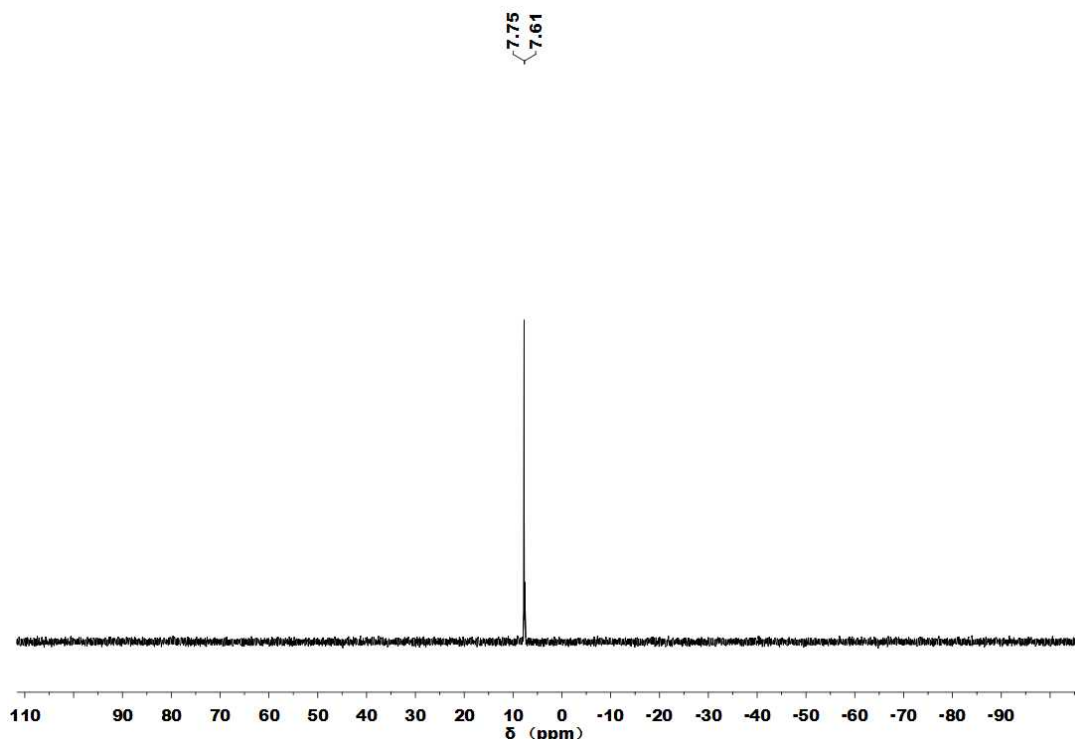


Figure S2. $^{31}\text{P}\{\text{H}\}$ NMR spectrum of **1** in C_6D_6 at 25 °C

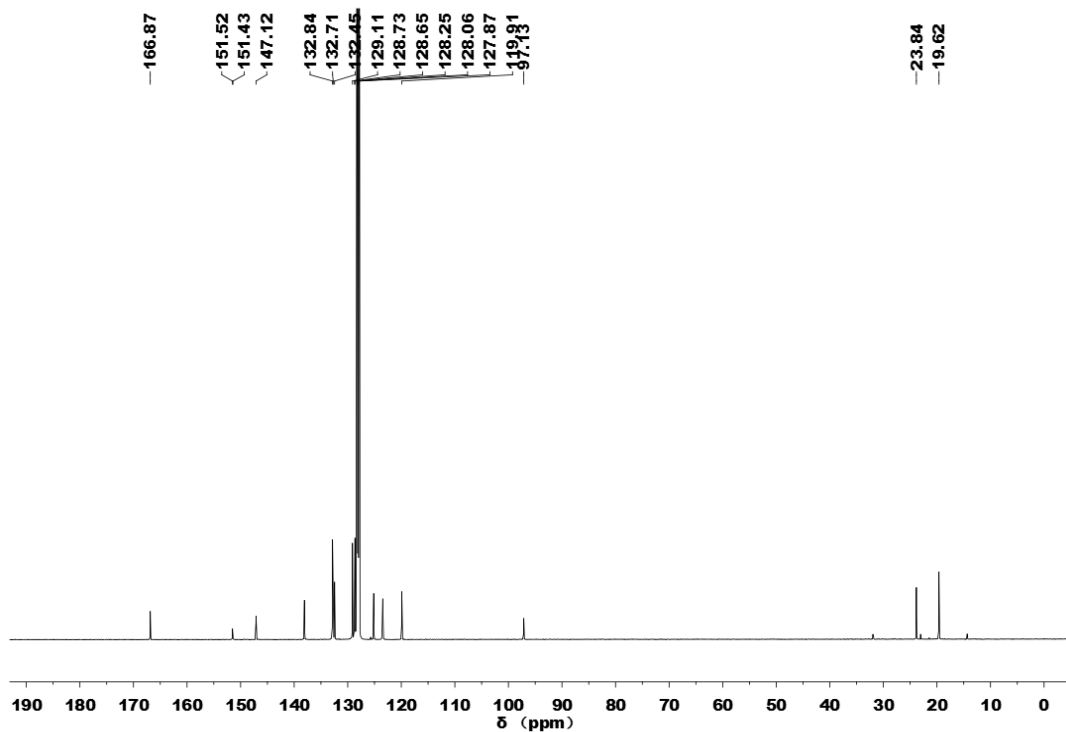


Figure S3. $^{13}\text{C}\{^1\text{H}\}$ NMR spectrum of **1** in C_6D_6 at 25°C .

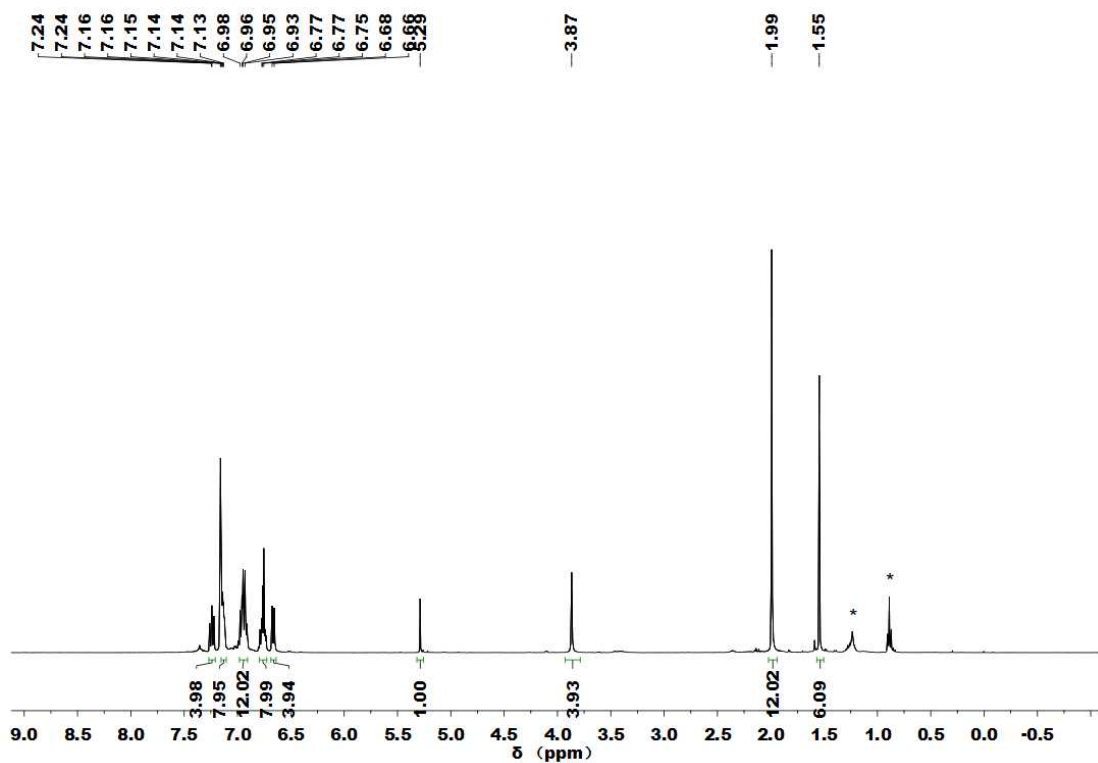


Figure S4. ^1H NMR spectrum of **2** in C_6D_6 at 25°C . (*) denotes small amount of hexane)

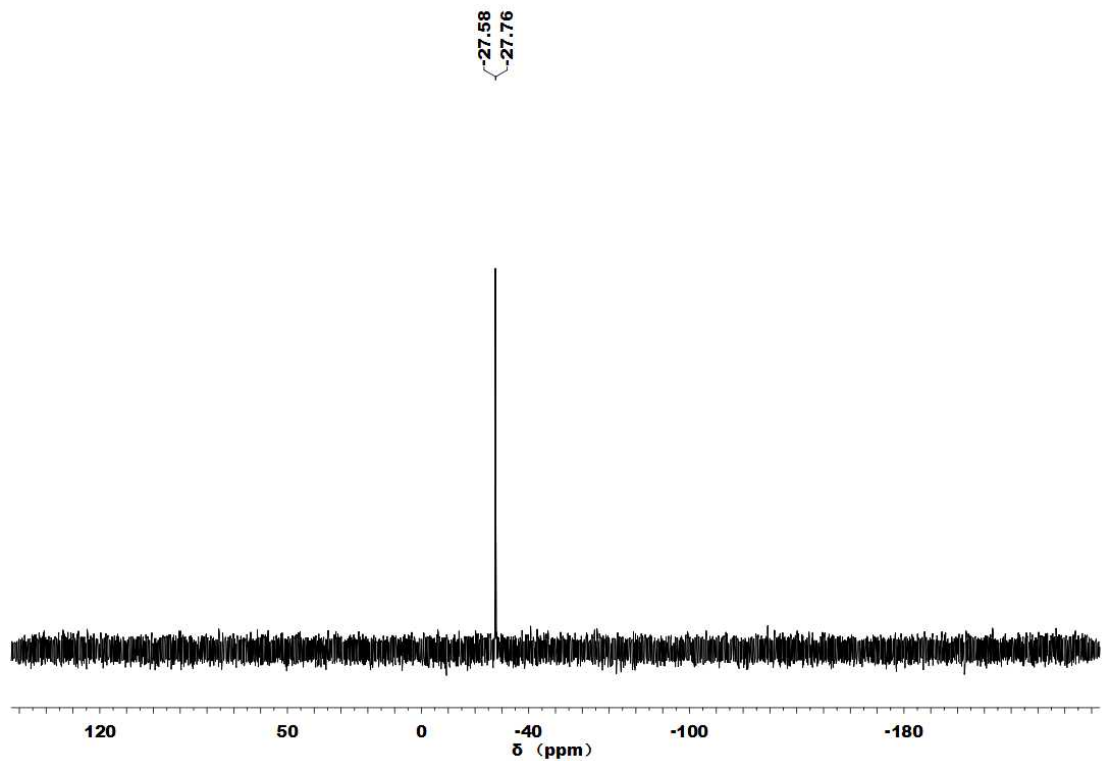


Figure S5. $^{31}\text{P}\{\text{H}\}$ NMR spectrum of **2** in C_6D_6 at 25 °C.

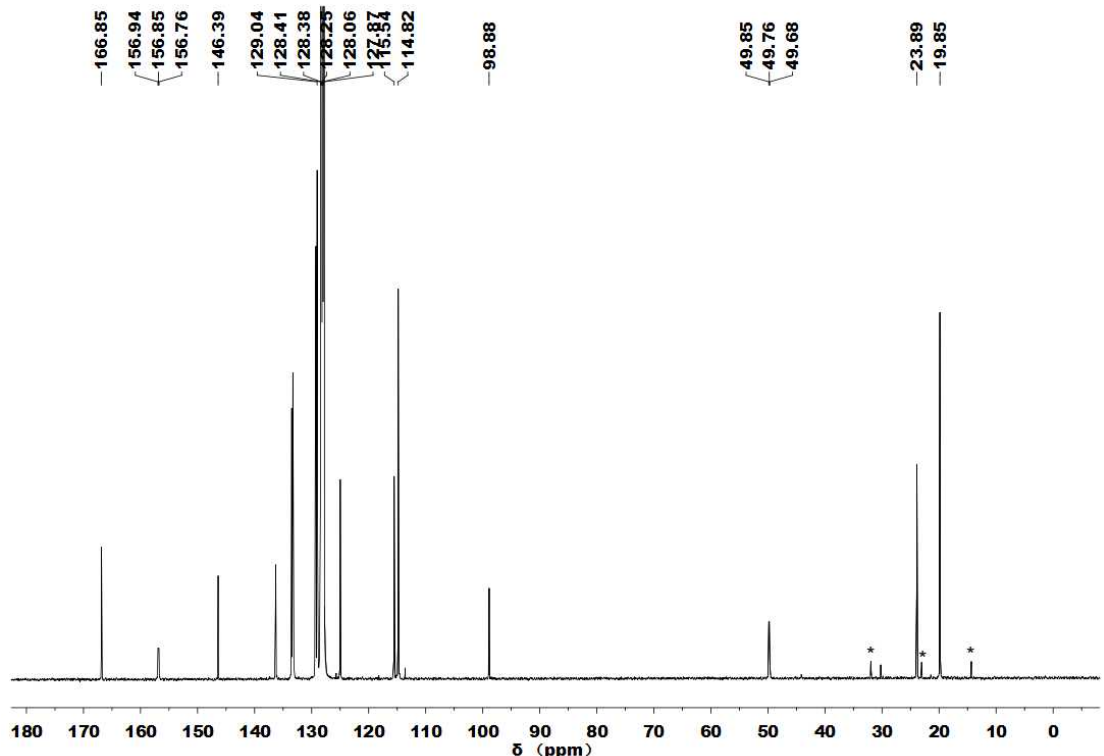


Figure S6. $^{13}\text{C}\{\text{H}\}$ NMR spectrum of **2** in C_6D_6 at 25 °C. (*) denotes small amount of hexane)

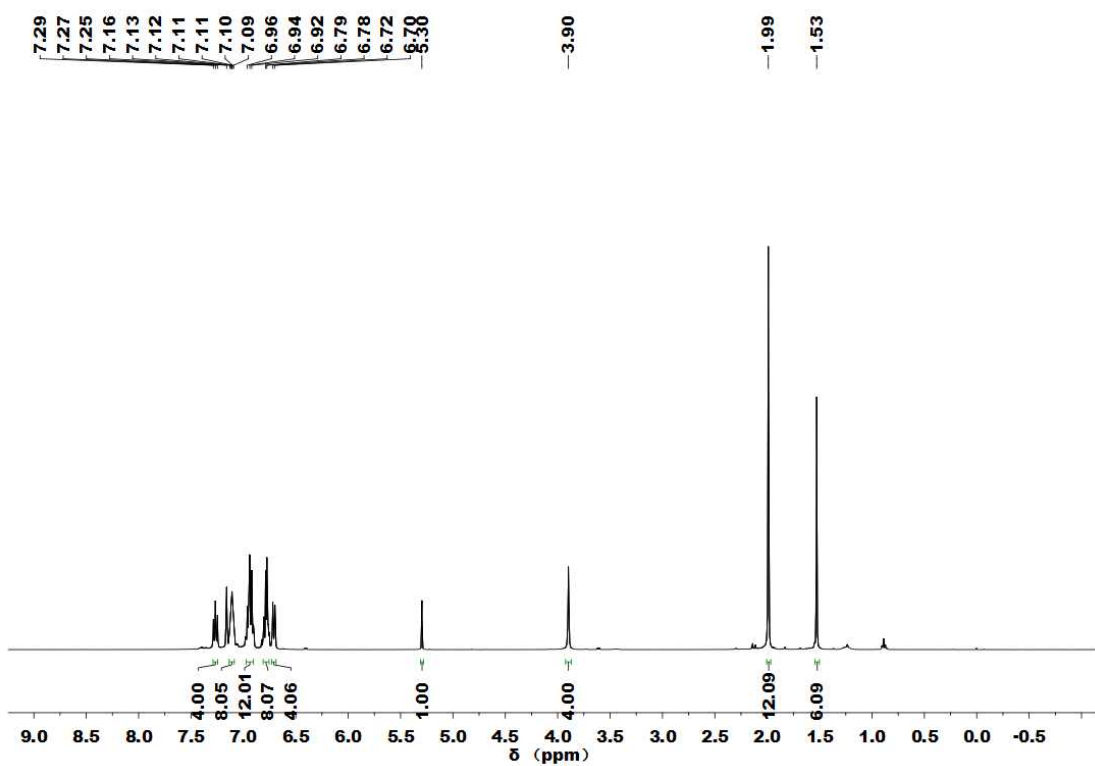


Figure S7. ¹H NMR spectrum of **3** in C₆D₆ at 25 °C.

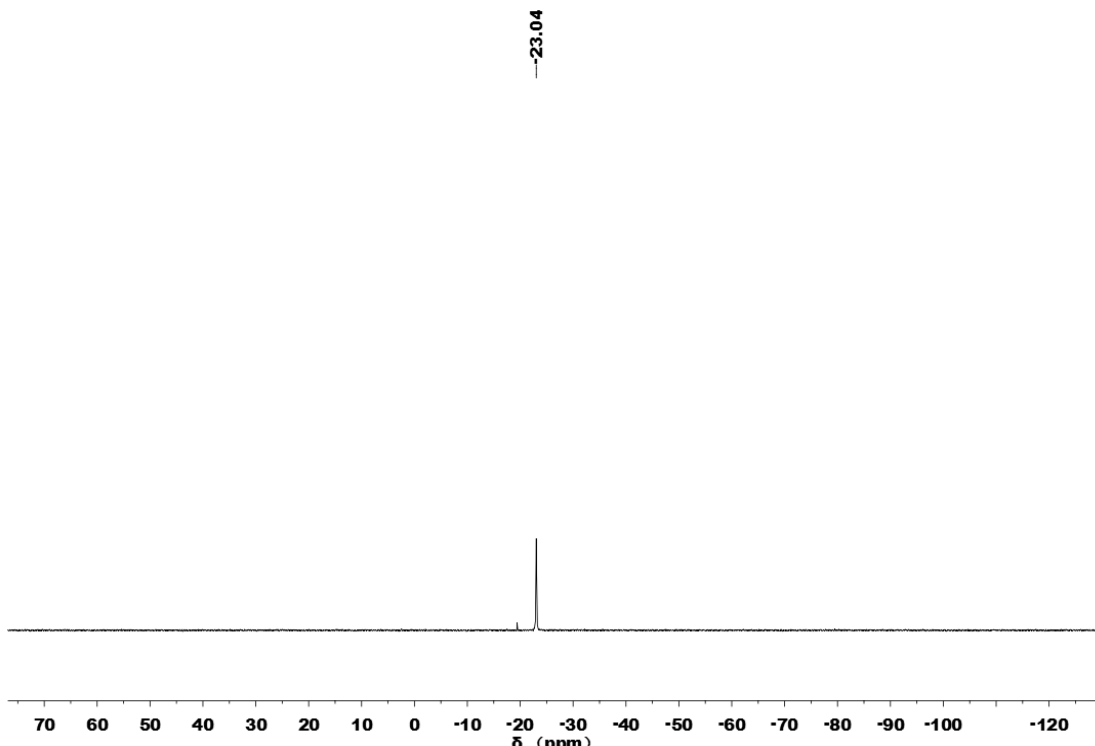


Figure S8. ³¹P{¹H} NMR spectrum of **3** in C₆D₆ at 25 °C.

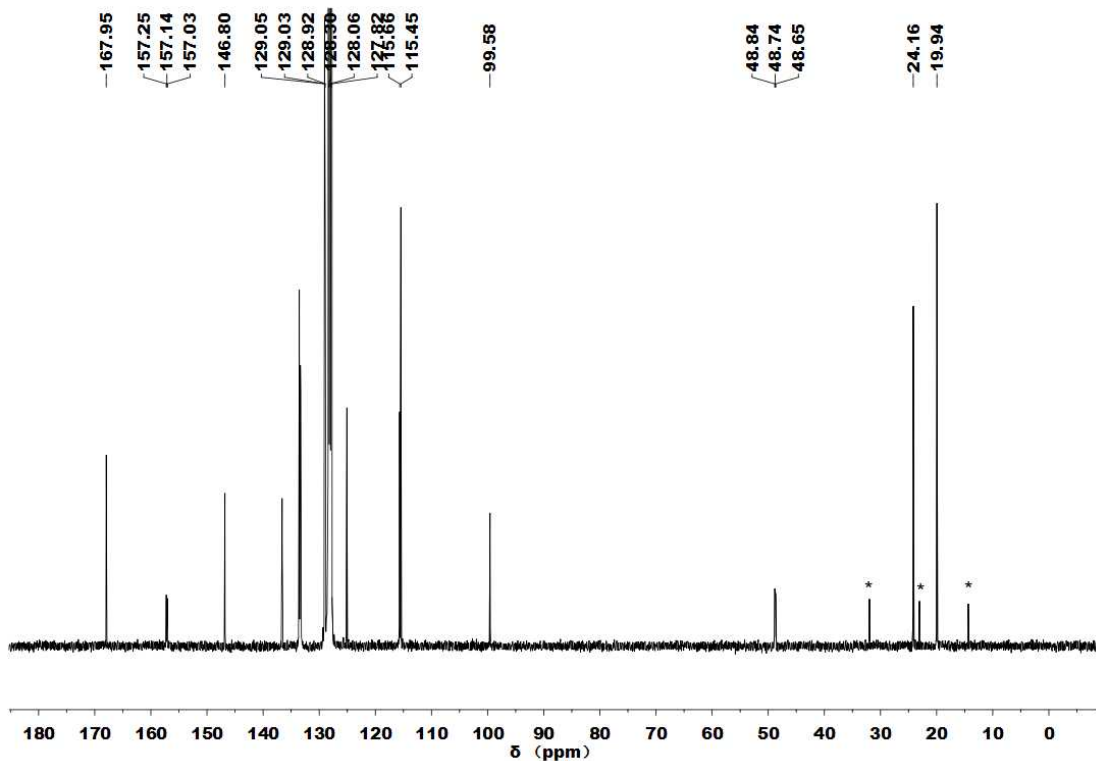


Figure S9. $^{13}\text{C}\{^1\text{H}\}$ NMR spectrum of **3** in C_6D_6 at $25\text{ }^\circ\text{C}$. (* denotes small amount of hexane)

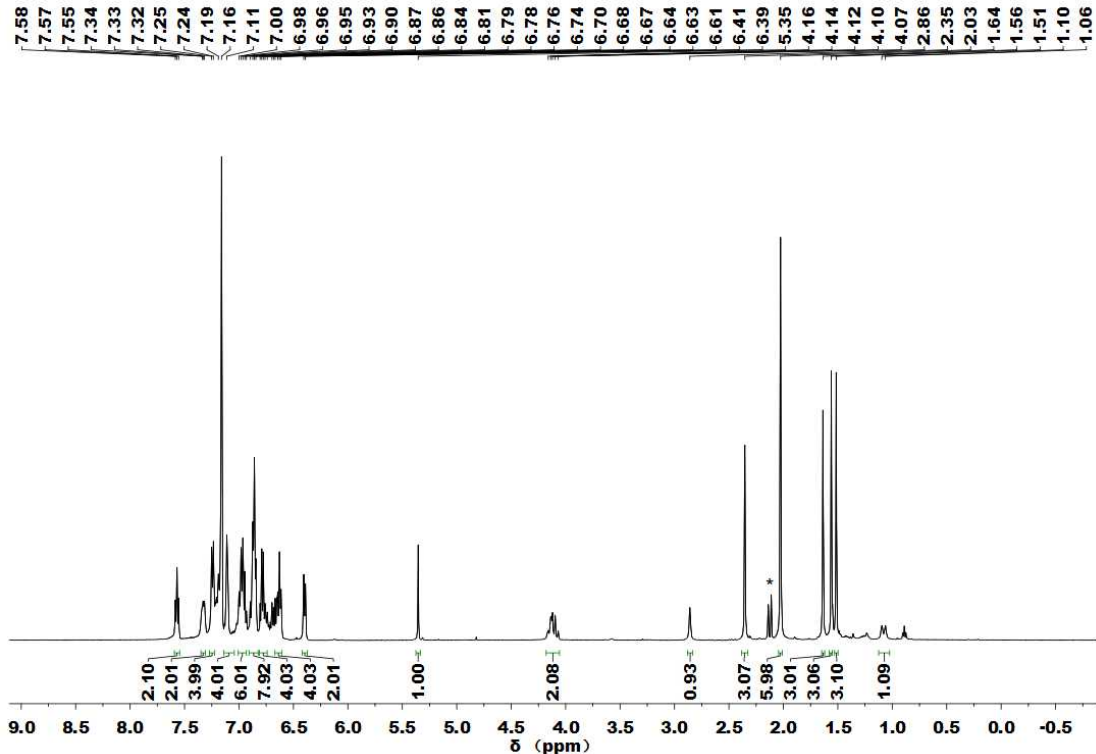


Figure S10. ^1H NMR spectrum of **4** in C_6D_6 at $25\text{ }^\circ\text{C}$. (* denotes small amount of toluene)

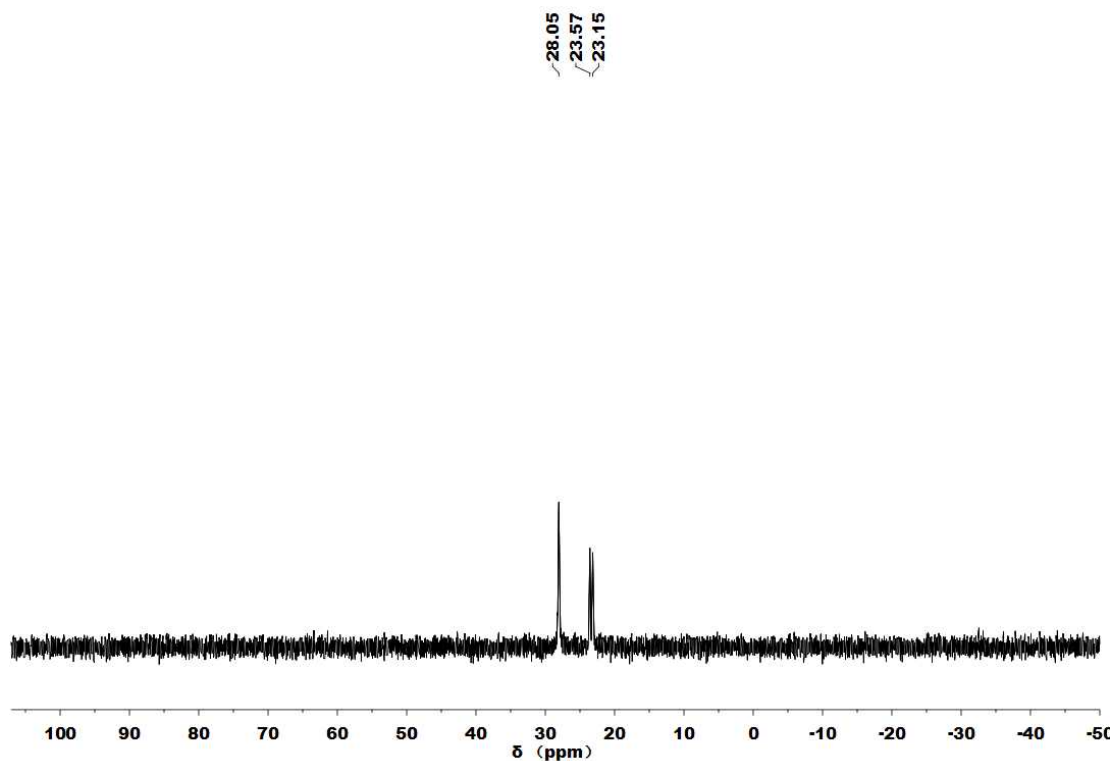


Figure S11. $^{31}\text{P}\{\text{H}\}$ NMR spectrum of **4** in C_6D_6 at 25°C .

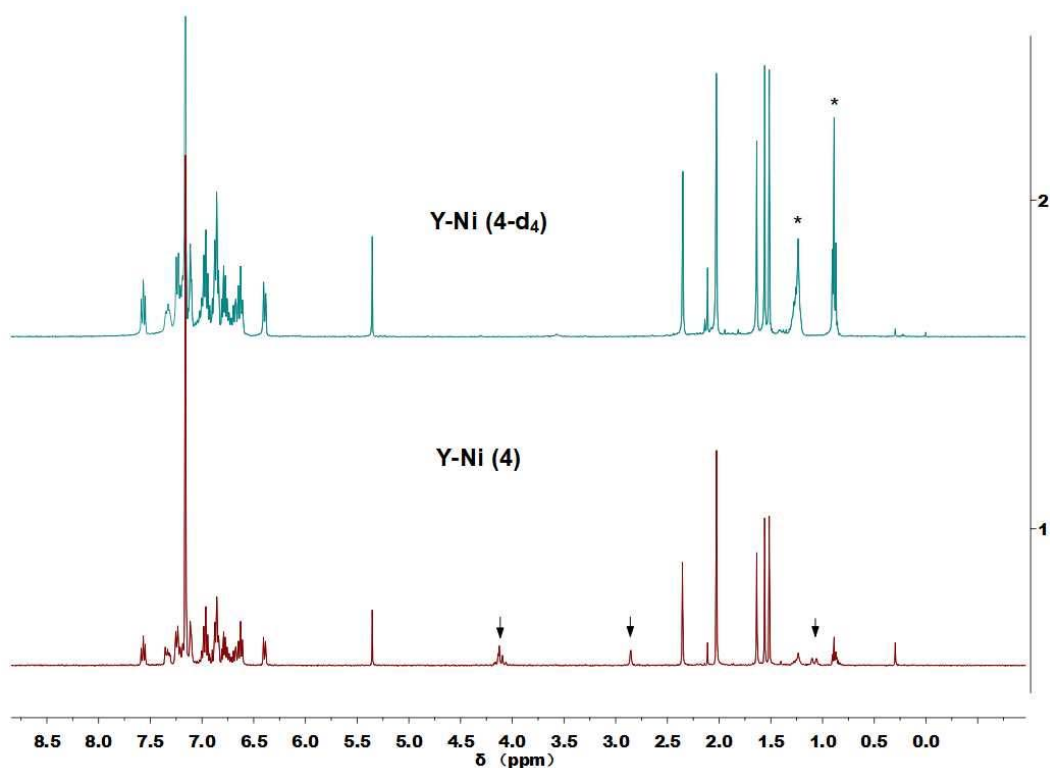


Figure S12. Stacked ^1H NMR spectra of **4** and $4-\text{d}_4$ in C_6D_6 at 25°C . (*) denotes small amount of hexane)

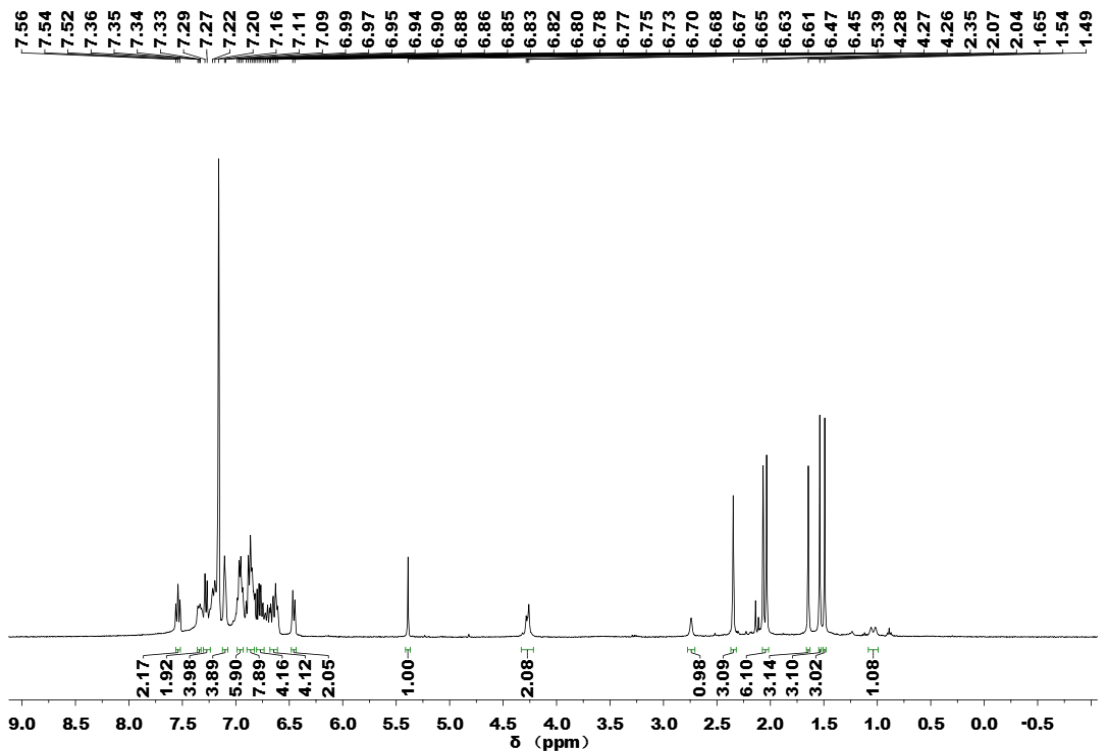


Figure S13. ^1H NMR spectrum of **5** in C_6D_6 at 25 °C.

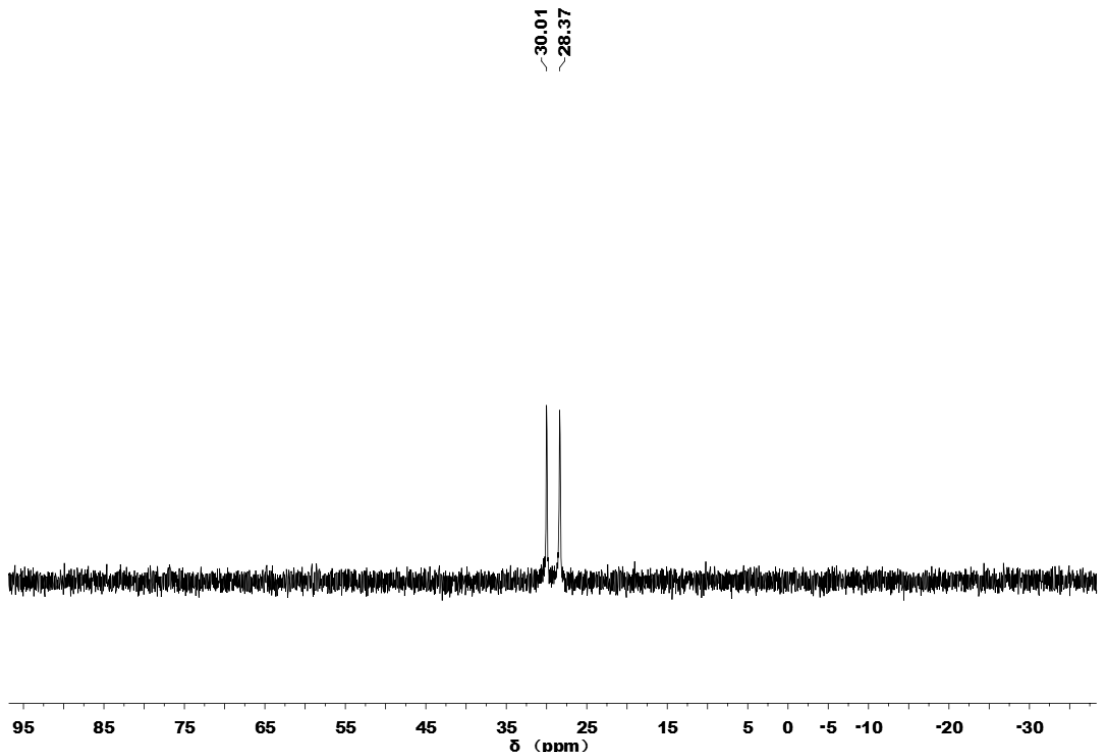


Figure S14. $^{31}\text{P}\{\text{H}\}$ NMR spectrum of **5** in C_6D_6 at 25 °C.

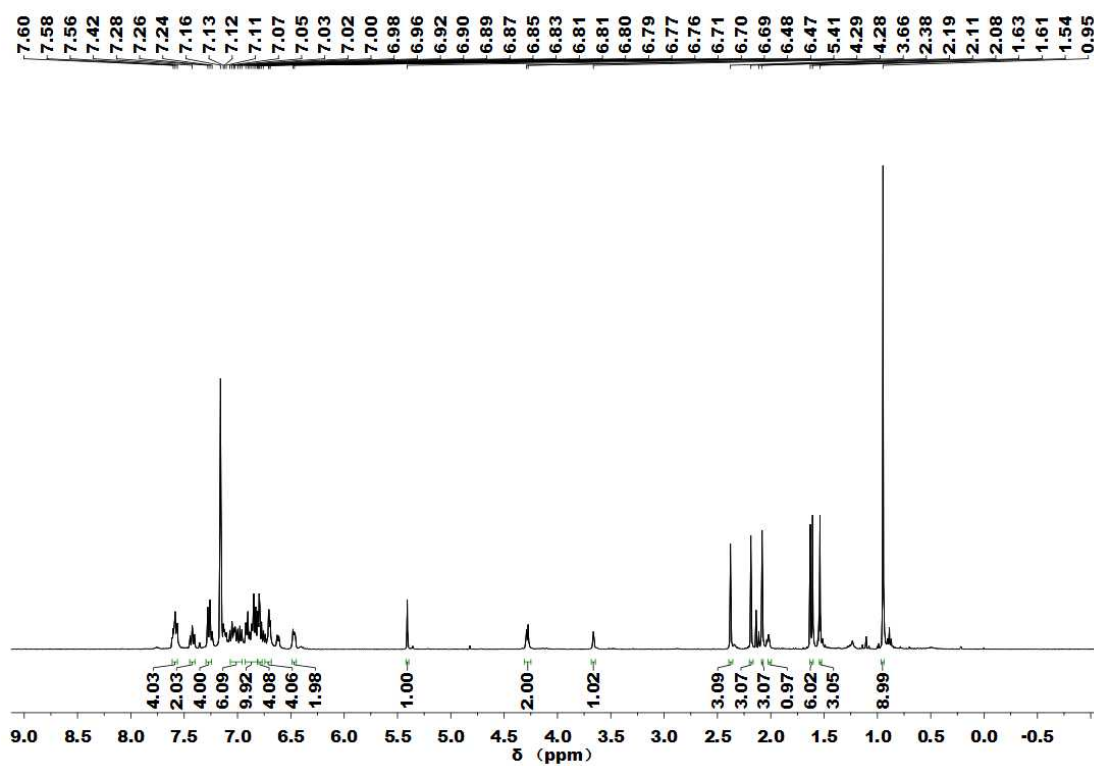


Figure S15. ^1H NMR spectrum of **6** in C_6D_6 at 25 °C.

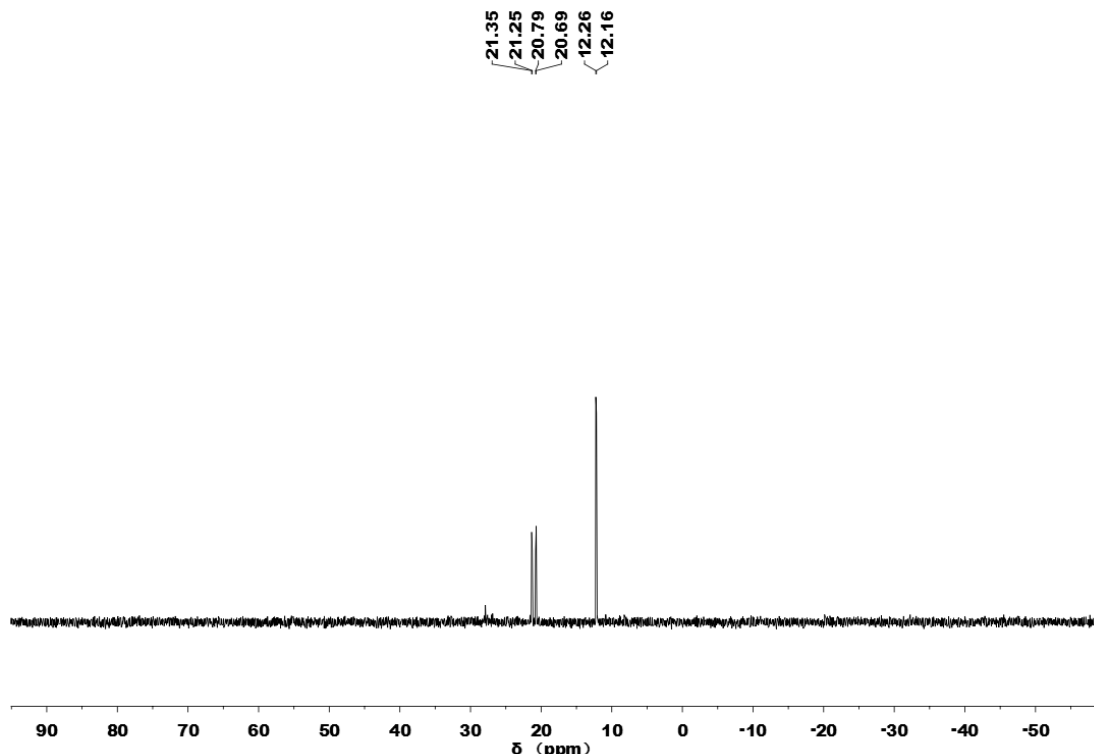


Figure S16. $^{31}\text{P}\{\text{H}\}$ NMR spectrum of **6** in C_6D_6 at 25 °C.

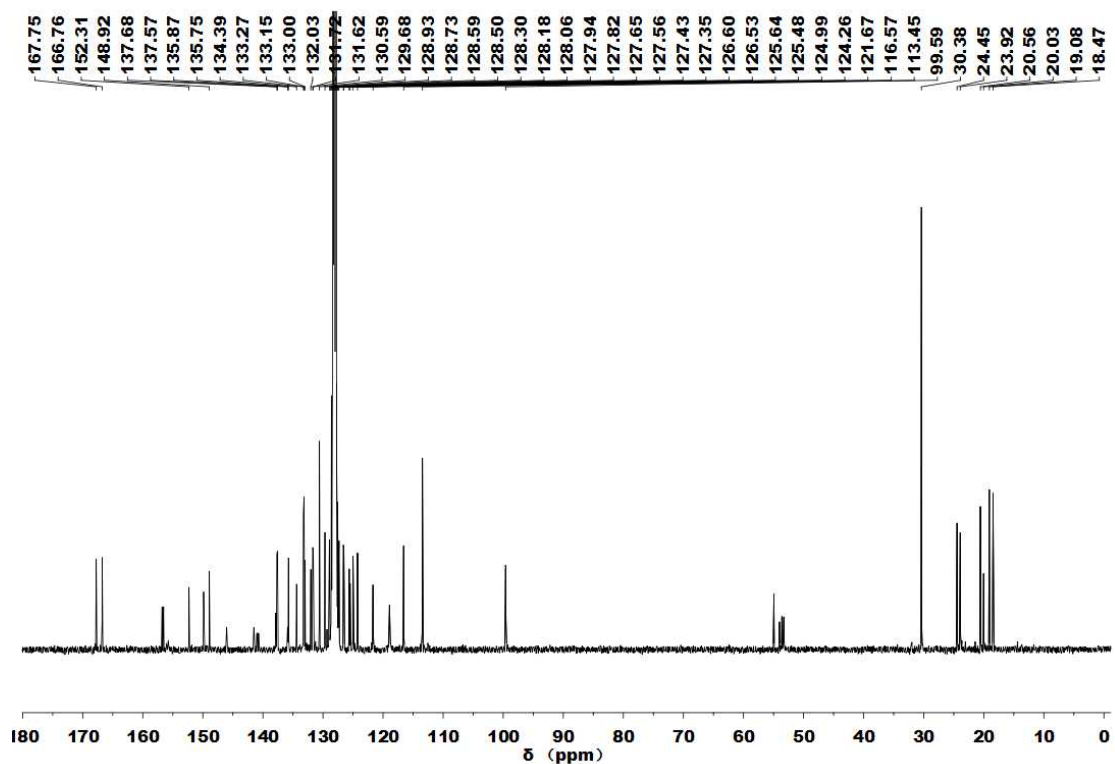


Figure S17. $^{13}\text{C}\{^1\text{H}\}$ NMR spectrum of **6** in C_6D_6 at 25°C .

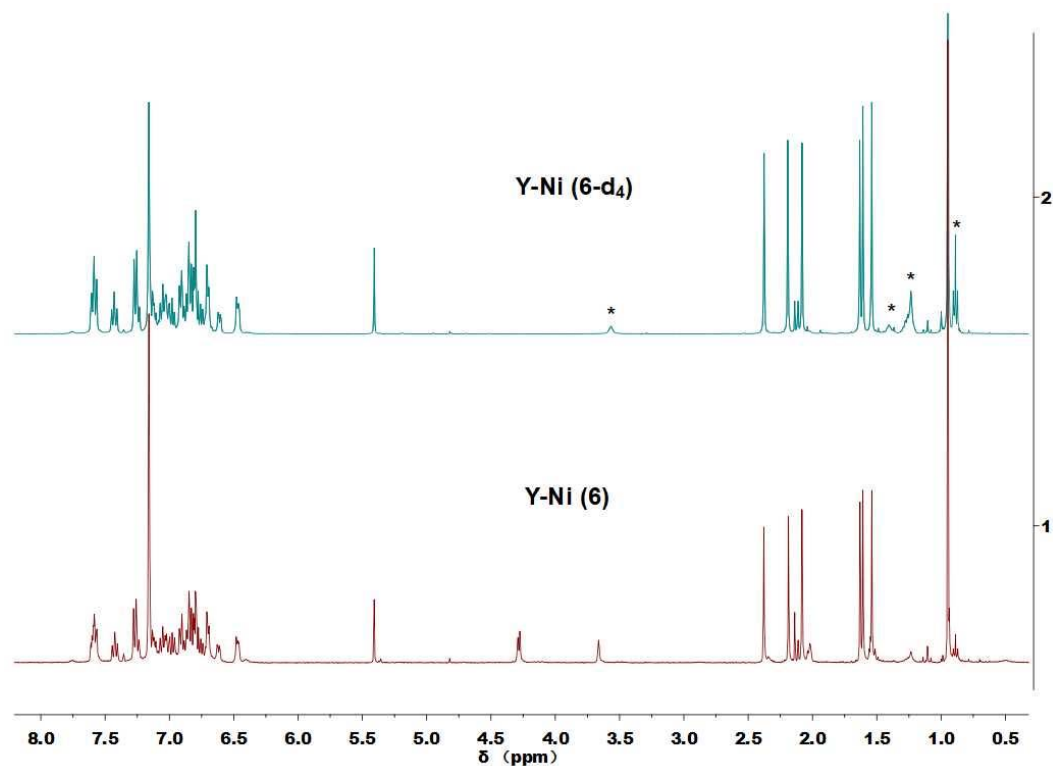


Figure S18. Stacked ^1H NMR spectra of **6** and **6-d₄** in C_6D_6 at 25°C . (*)denotes small amount of THF and hexane)

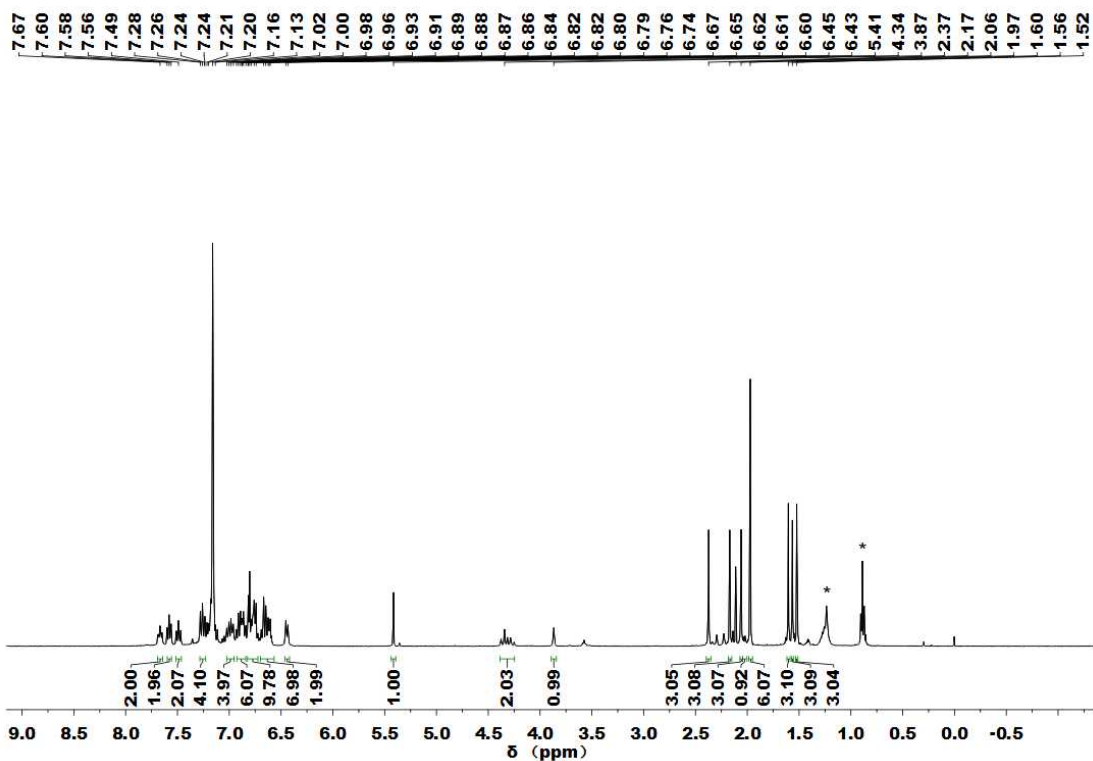


Figure S19. ^1H NMR spectrum of **7** in C_6D_6 at $25\text{ }^\circ\text{C}$. (*) denotes small amount of hexane)

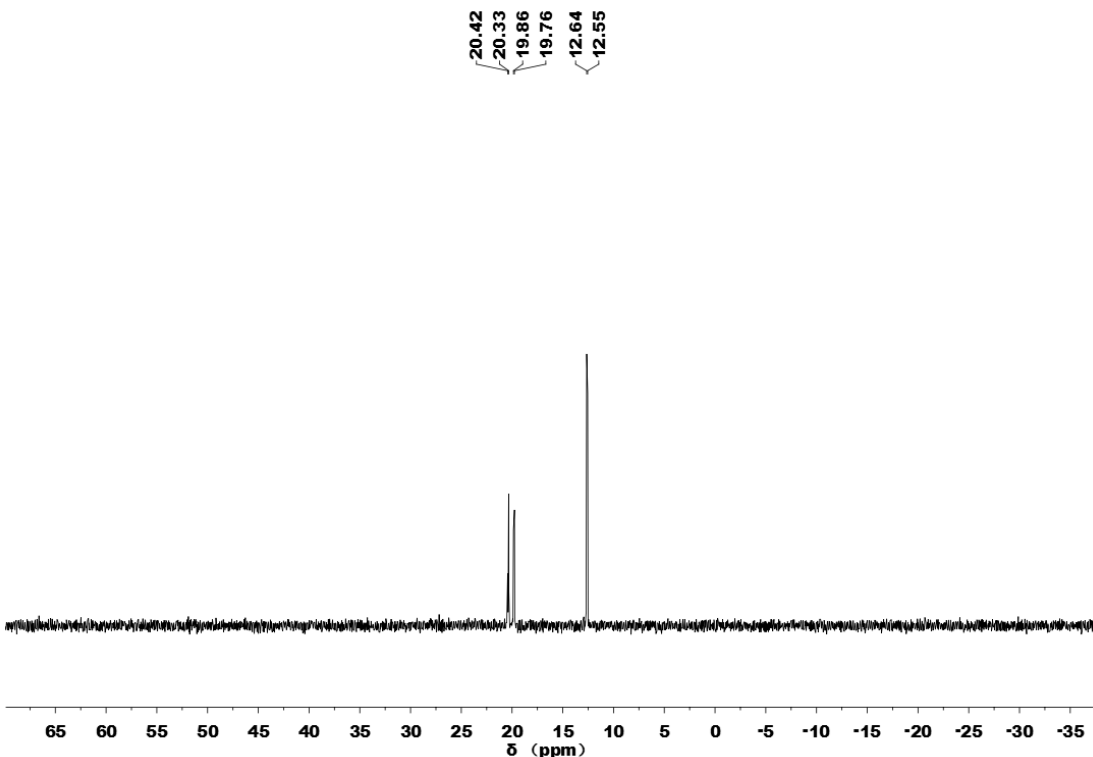


Figure S20. $^{31}\text{P}\{^1\text{H}\}$ NMR spectrum of **7** in C_6D_6 at $25\text{ }^\circ\text{C}$.

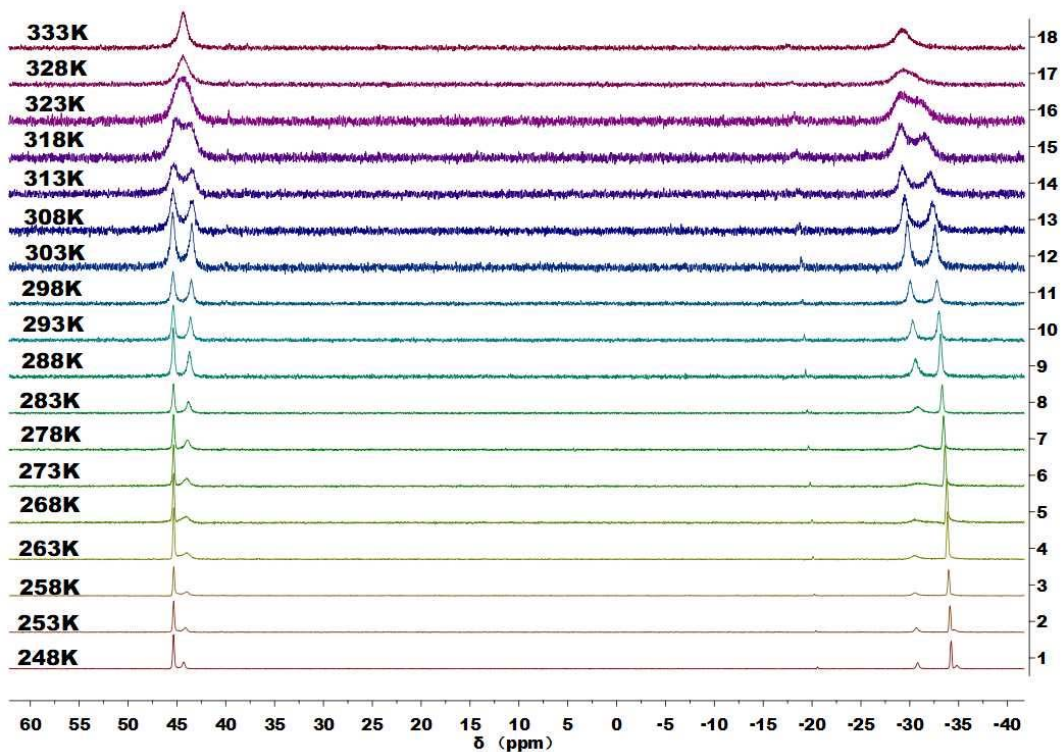


Figure S21. VT-³¹P{¹H} NMR spectra of **8** in toluene-*d*8 at various temperature (248-333K).

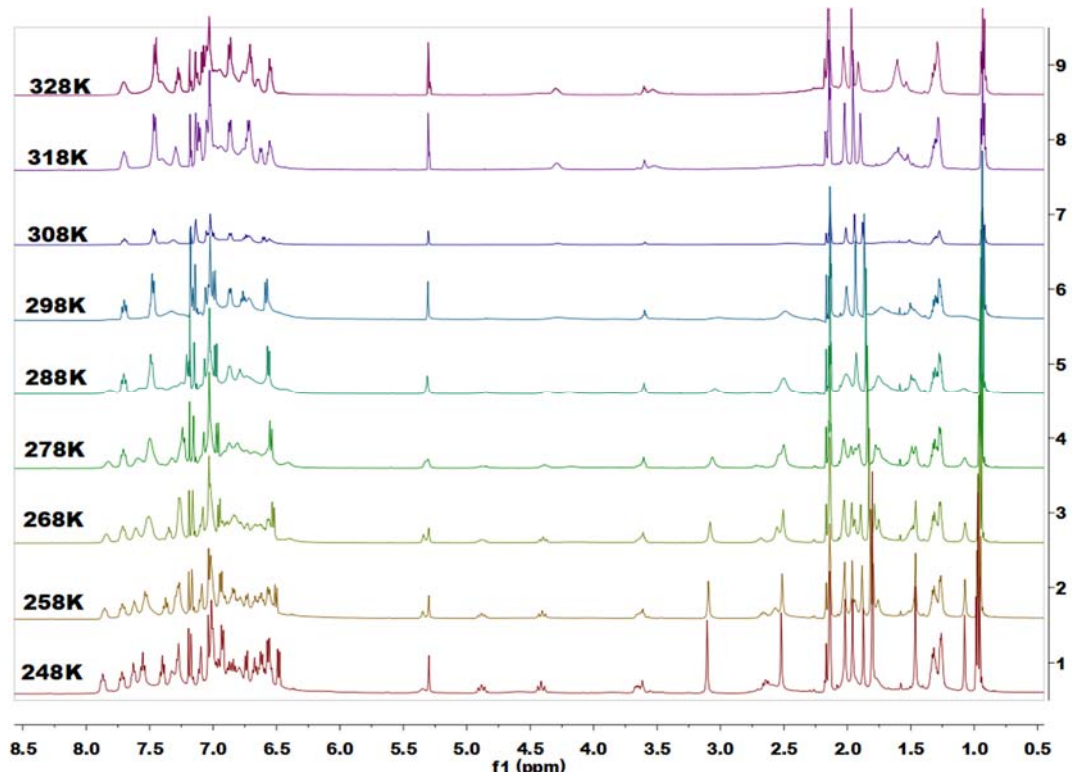


Figure S22. VT-¹H NMR spectra of **8** in toluene-*d*8 at various temperature (248-328K).

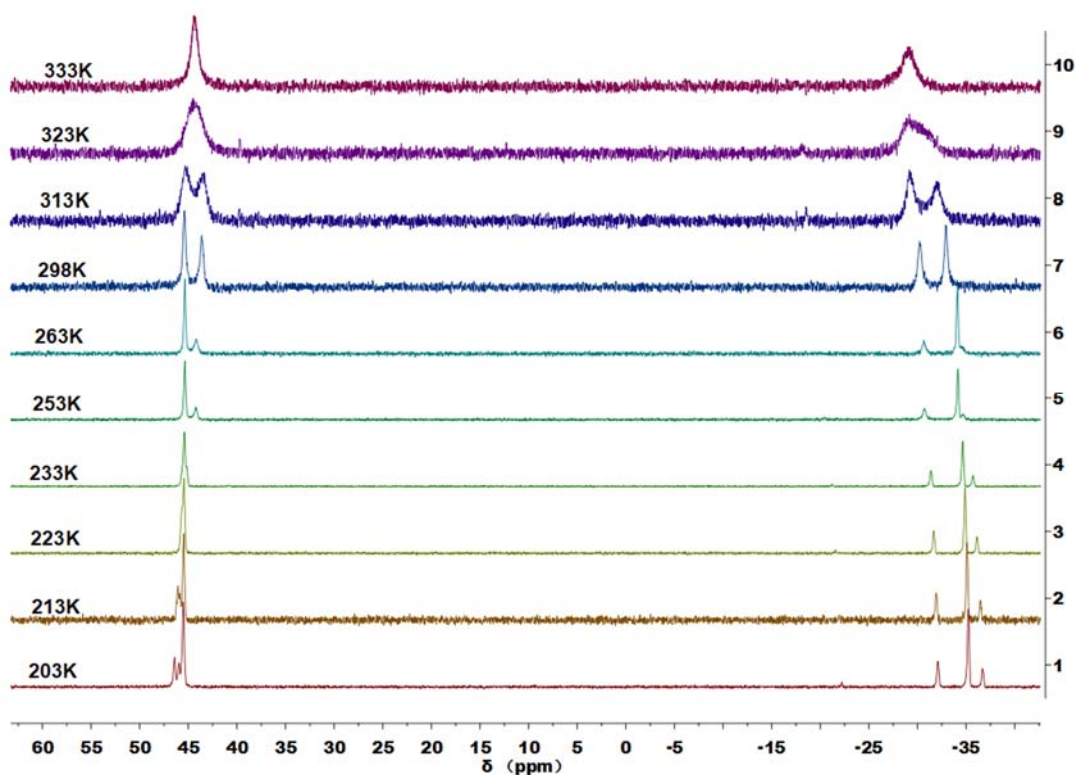


Figure S23. VT- $^{31}\text{P}\{\text{H}\}$ NMR spectra of **8** in toluene- d_8 at various temperature (203-333K).

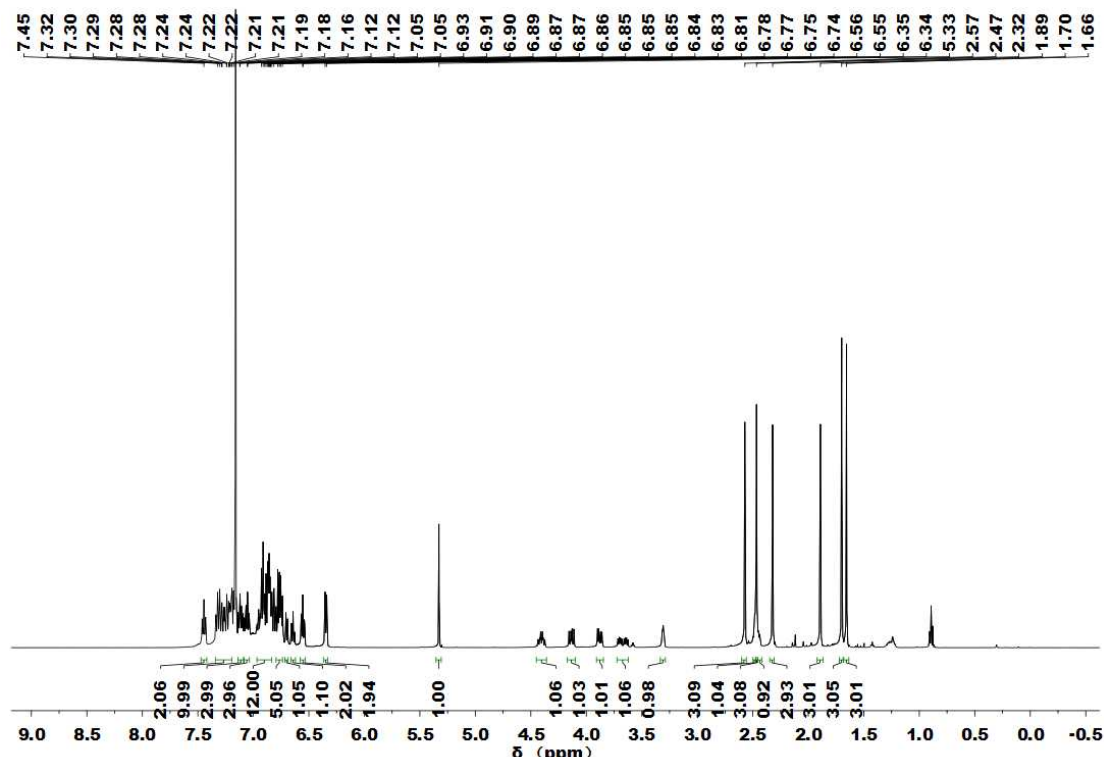


Figure S24. ^1H NMR spectrum of **9** in C_6D_6 at 25 °C.

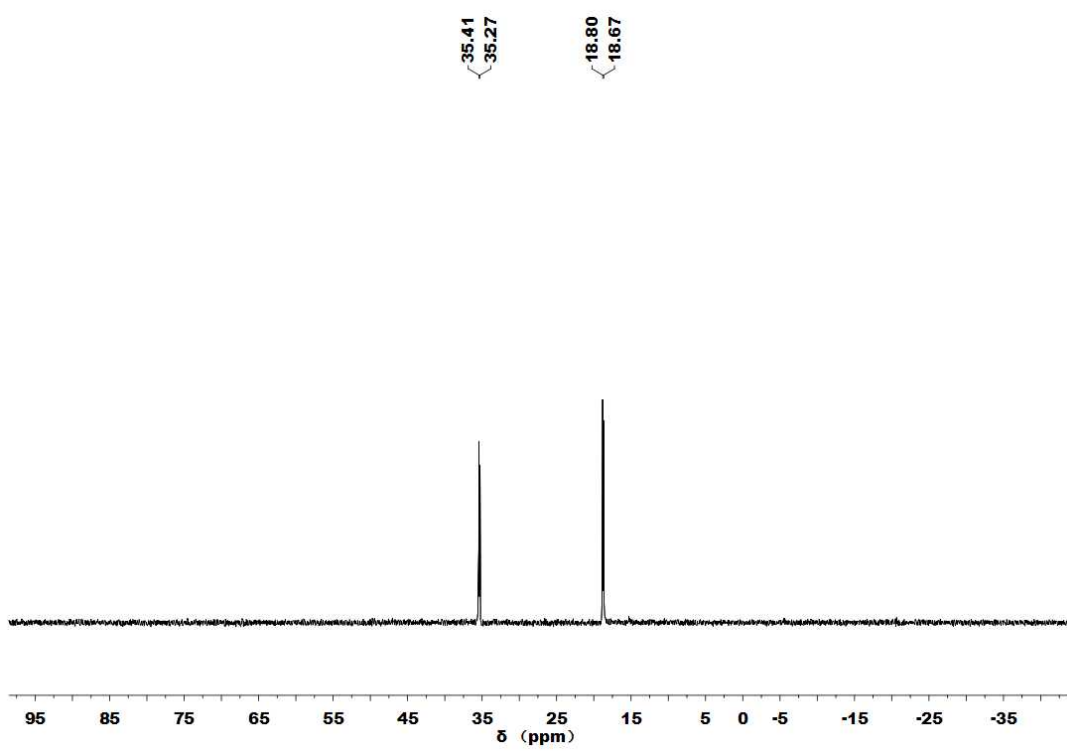


Figure S25. $^{31}\text{P}\{\text{H}\}$ NMR spectrum of **9** in C_6D_6 at 25 °C.

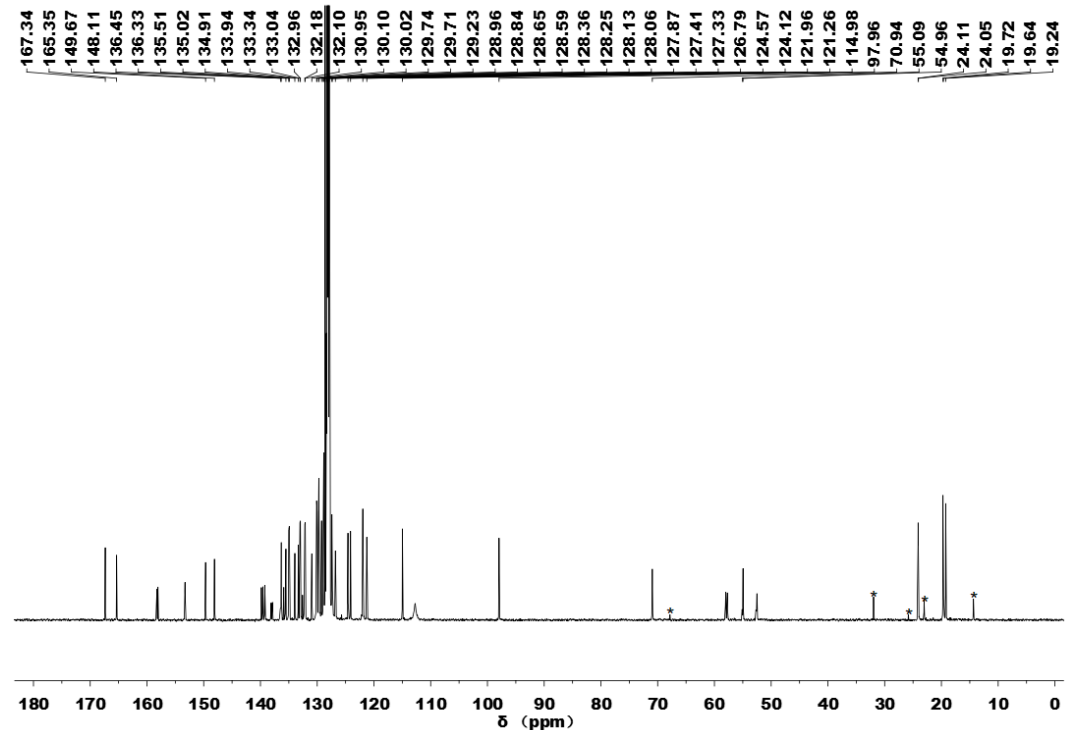


Figure S26. $^{13}\text{C}\{\text{H}\}$ NMR spectrum of **9** in C_6D_6 at 25 °C. (*) denotes small amount of THF and hexane)

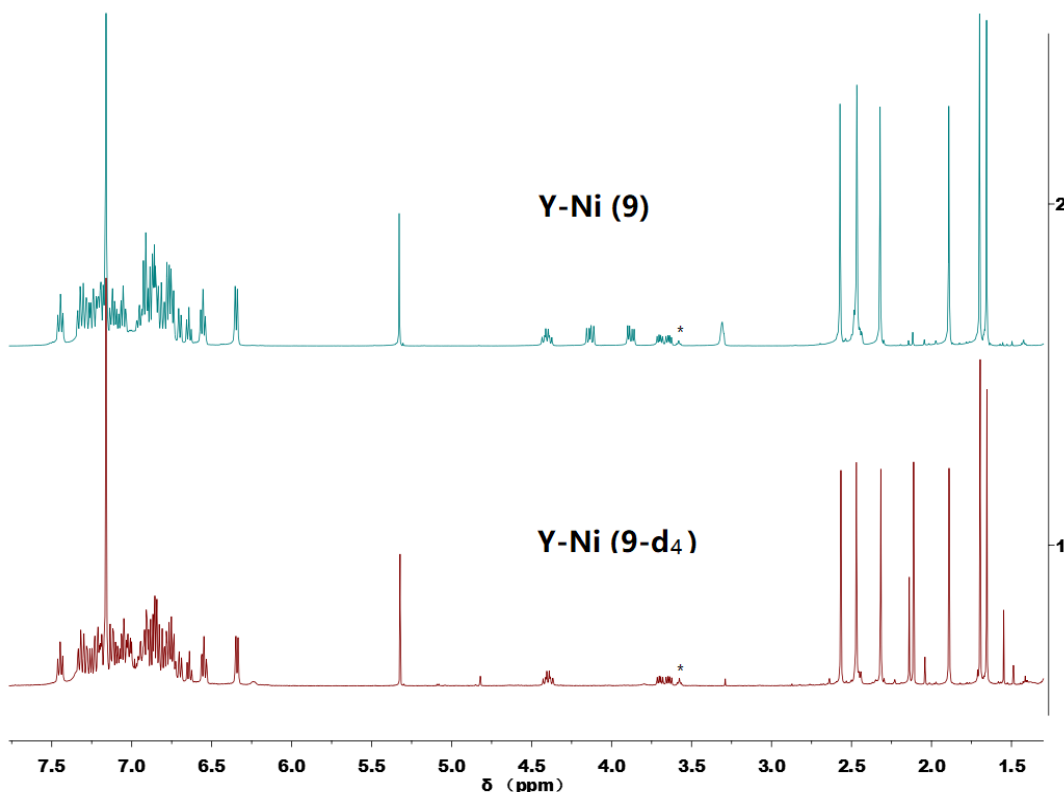


Figure S27. Stacked ^1H NMR spectra of **9** and **9- d_4** in C_6D_6 at 25 °C. (*denotes small amount of THF)

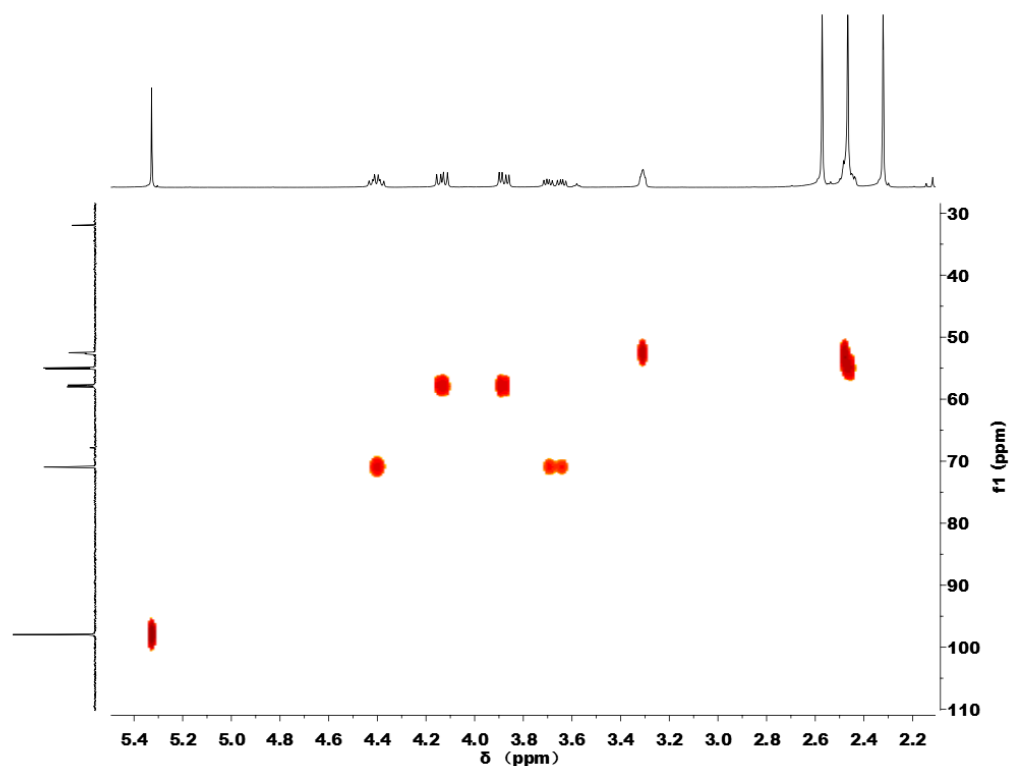


Figure S28. HSQC spectrum of **9**

1.2. IR Spectra

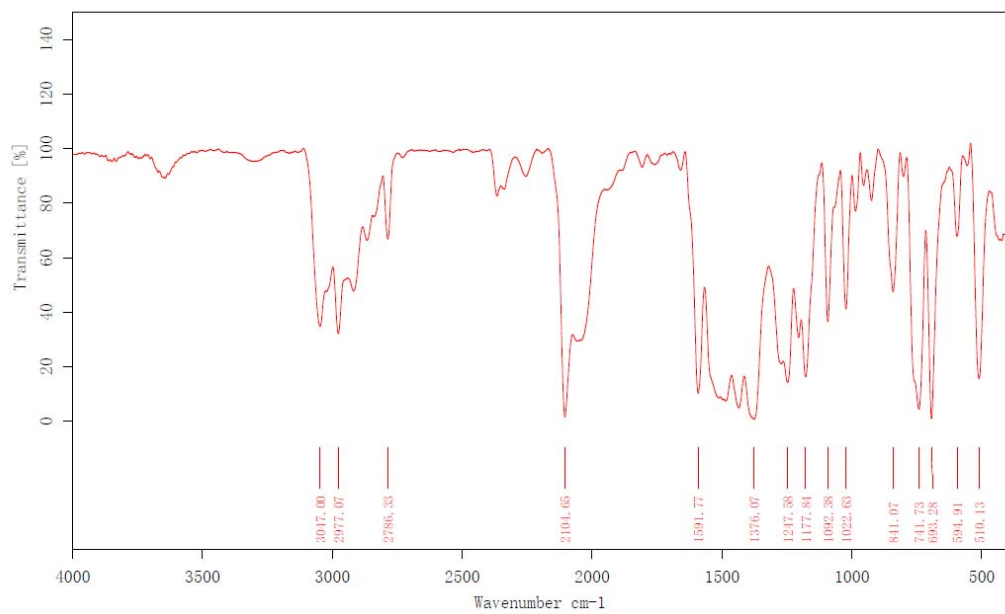


Figure S29. IR spectrum of solid 6.

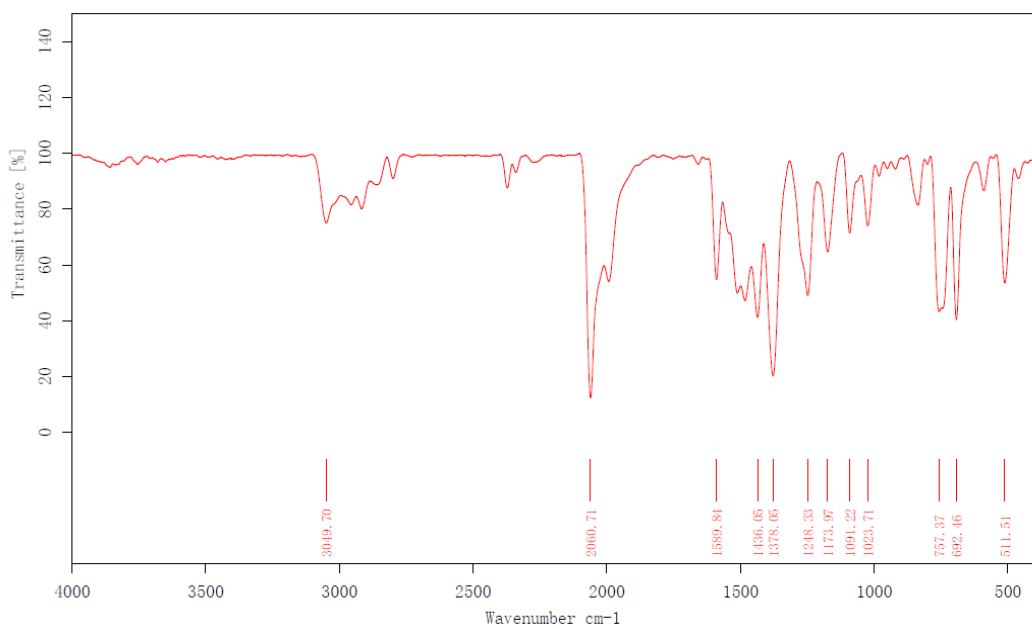


Figure S30. IR spectrum of solid 7.

2. X-ray Crystallography

X-ray Crystallography. Diffraction was performed on a Bruker SMART APEX II CCD area detector diffractometer using graphite-monochromated Mo $K\alpha$ radiation ($\lambda = 0.71073 \text{ \AA}$) and Bruker Platn II area detector diffractometer using graphite-monochromated Mo $K\alpha$ radiation ($\lambda = 0.71073 \text{ \AA}$) for complexes, φ and ω scan technique. An empirical absorption correction was applied using the SADABS program.¹ All structures were solved by direct methods, completed by subsequent difference Fourier syntheses, and refined anisotropically for all non-hydrogen atoms by full-matrix least-squares calculations based on F^2 using the SHELXTL program package² and Olex 2 program⁴. The hydrogen atom coordinates were calculated with SHELXTL by using an appropriate riding model with varied thermal parameters. The residual electron densities of solvent were squeezed by using PLATON.³ All crystal structural pictures drawn by Olex 2 program.⁴ Crystal parameters and refinement results are given in Table S1-S2.

Table S1. Crystallographic and Refinement Data ^{a,b} for **1, 2, 4, 5**

	1	2	4	5
formula	$C_{57}H_{55}N_4P_2Y$	$C_{59}H_{59}N_4P_2Y$	$C_{59}H_{59}N_4P_2NiY$	$C_{59}H_{59}N_4P_2NiLu$
$F_w, \text{g}\cdot\text{mol}^{-1}$	946.90	974.95	1033.66	1119.72
cryst size, mm	0.22 x 0.21 x 0.2	0.21 x 0.2 x 0.18	0.21 x 0.19 x 0.18	0.22 x 0.20 x 0.19
cryst. syst.	triclinic	monoclinic	triclinic	triclinic
space group	P -1	P 1 21/n 1	P -1	P -1
T, K	273(2)	273(2)	273(2)	300(2)
$a, \text{\AA}$	12.168(2)	13.7148(8)	12.1820(5)	12.2096(6)
$b, \text{\AA}$	12.969(2)	19.1621(13)	12.4634(5)	12.4762(7)
$c, \text{\AA}$	17.303(3)	20.6907(13)	19.2026(7)	19.1394(10)
$\alpha, {}^\circ$	84.336(6)	90	82.367(2)	82.165(2)
$\beta, {}^\circ$	72.086(6)	108.426(2)	76.584(2)	76.565(2)
$\gamma, {}^\circ$	73.669(6)	90	64.7460(10)	64.391(2)
$V, \text{\AA}^3$	2493.1(8)	5158.8(6)	2563.01(18)	2555.0(2)
Z	2	4	2	2
$D_{\text{calcd}}, \text{Kg}\cdot\text{m}^{-3}$	1.261	1.255	1.339	1.455
$F(000)$	988.0	2040.0	1076.0	1140.0
μ, mm^{-1}	1.275	1.234	1.598	2.394
θ range / $^\circ$	2.949 - 25.039	2.971 - 27.815	2.888 - 27.564	2.899 - 27.537
refns collected	8659	207071	132946	71865
indep reflns (R_{int})	8659	11995 (0.0718)	11820 (0.0594)	11738 (0.0501)
reflns obsd [$I > 2\sigma(I)$]	7609	8848	9315	9914
data/restrnts/params	8659 / 1216 / 488	11995 / 1284 / 601	11820 / 1323 / 610	11738 / 1308 / 610
$R1, wR2 (I > 2\sigma(I))$	0.1224, 0.3296	0.0545, 0.1376	0.0440, 0.1076	0.0319, 0.0624
$R1, wR2$ (all data)	0.1324, 0.3345	0.0832, 0.1608	0.0644, 0.1197	0.0466, 0.0681
GOF on F2	1.125	1.083	1.047	1.037
$\Delta\rho_{\text{max}, \text{min}}, \text{e}\cdot\text{\AA}^{-3}$	2.274, -1.933	0.721, -0.418	0.644, -0.657	0.849, -0.801

^a $R1 = \Sigma|F_o| - |F_c|/\Sigma|F_o|$. ^b $wR2 = \{\sum w(F_o^2 - F_c^2)^2 / \sum w(F_o^2)\}^{1/2}$.

Table S2. Crystallographic and Refinement Data ^{a,b} for **6-9**

	6	7	8	9
formula	C ₆₄ H ₆₈ N ₅ P ₂ NiY	C ₆₈ H ₆₈ N ₅ NiP ₂ Y	C ₇₅ H ₇₃ N ₆ NiP ₂ Y	C ₆₇ H ₆₇ N ₄ NiOP ₂ Y·C ₇ H ₈
Fw, g·mol ⁻¹	1116.79	1164.83	1267.95	1245.94
cryst size, mm	0.22 x 0.21 x 0.2			
cryst. syst.	monoclinic	triclinic	monoclinic	triclinic
space group	P 1 21/n 1	P -1	P 1 21/c 1	P -1
T, K	273(2)	273(2)	273(2)	293(2)
<i>a</i> , Å	12.2206(19)	12.443(4)	14.384(3)	14.533(5)
<i>b</i> , Å	22.319(4)	12.656(4)	20.649(4)	15.248(5)
<i>c</i> , Å	21.549(3)	23.095(9)	21.706(4)	16.887(6)
α , °	90	82.321(11)	90	86.604(4)
β , °	97.461(5)	82.700(11)	92.10(3)	80.637(4)
γ , °	90	64.088(10)	90	62.662(4)
<i>V</i> , Å ³	5827.8(16)	3232(2)	6443(2)	3279.5(19)
Z	4	2	4	2
<i>D</i> _{calcd} , Kg·m ⁻³	1.273	1.197	1.307	1.262
<i>F</i> (000)	2336.0	1216.0	2648	1304
μ , mm ⁻¹	1.412	1.275	1.286	1.262
θ range /°	2.851 -24.998	2.830 - 24.999	2.985 - 28.722	1.504 - 25.064
refns collected	101045	205675	148216	11330
indep reflns (<i>R</i> _{int})	10248 (0.1993)	11357 (0.1649)	15008 (0.0853)	11330
reflns obsd [<i>I</i> > 2σ(<i>I</i>)]	6408	7778	10320	7895
data/restrnts/params	10248/1425/631	11357/1519/702	15008/1764/774	11330/1618/720
<i>R</i> 1, <i>wR</i> 2 (<i>I</i> > 2σ(<i>I</i>))	0.1107, 0.2722	0.0647, 0.1344	0.0588, 0.1377	0.1265, 0.3446
<i>R</i> 1, <i>wR</i> 2 (all data)	0.1737, 0.3210	0.1081, 0.1638	0.0958, 0.1573	0.1639, 0.3628
GOF on F2	1.126	1.056	1.013	1.084
Δρ _{max, min} , e·Å ⁻³	0.953, -0.748	0.425, -0.601	0.476, -0.451	1.704, -1.355

$$^a R1 = \sum |F_o| - |F_c| / \sum |F_o|. \quad ^b wR2 = \{ \sum w(F_o^2 - F_c^2)^2 / \sum w(F_o^2)^2 \}^{1/2}.$$

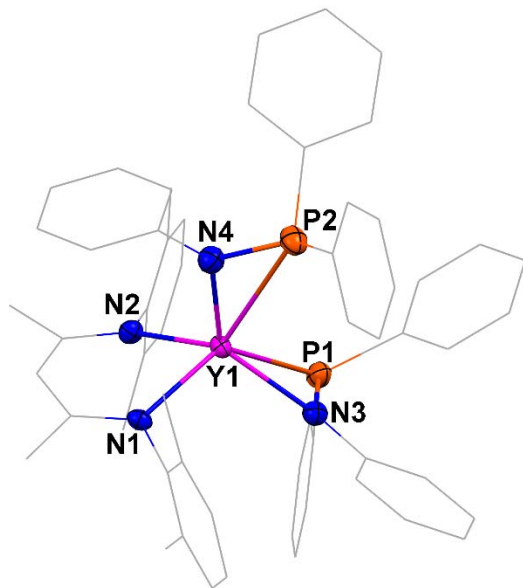


Figure S31. Molecular structure of **1** at the 30% thermal ellipsoids probability.

Hydrogen atoms were omitted for clarity.

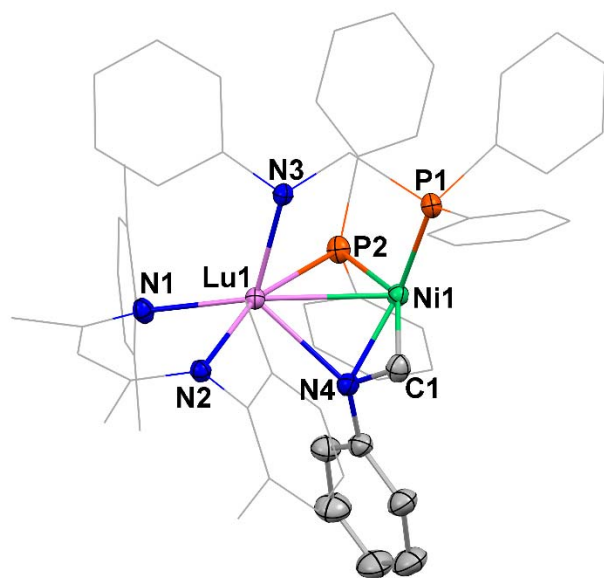


Figure S32. Molecular structure of **5** at the 30% thermal ellipsoids probability.

Hydrogen atoms were omitted for clarity.

3. References

1. Sheldrick G. M. *SADABS: Program for Empirical Absorption Correction of Area Detector Data*; University of Göttingen: Germany (1996).
2. Sheldrick G. M. *SHELXT*-Integrated space-group and crystalstructure determination. *Acta Cryst.* **A71**, 3-8 (2015).
3. Spek A. L. *PLATON SQUEEZE*: a tool for the calculation of the disordered solvent contribution to the calculated structure factors. *Acta Cryst.* **C71**, 9-18 (2015).
4. Dolomanov, O. V., Bourhis, L. J., Gildea, R. J., Howard, J. A. K. and Puschmann, H. *J. Appl. Crystallogr.* **2009**, 42, 339-341.